Xe 5s,5p correlation satellites in the region of strong interchannel interactions, 28–75 eV

Anders Fahlman,* Manfred O. Krause, Thomas A. Carlson, and Agneta Svensson†
Oak Ridge National Laboratory, Oak Ridge, Tennessee 37831
(Received 21 March 1984)

The Xe 5s,5p photoelectron satellite spectrum has been studied in the photon-energy range from 28 to 75 eV with the aid of synchrotron radiation. This range includes the Xe 5s Cooper minimum, and the cross sections and angular distribution data demonstrate the importance of the strong two-electron channels in the region where the 5s cross section is small. Although the behavior of the satellites was not recorded over the 4d maximum, the data near 75 eV show an enhancement in the cross section in that region. The data underline the need of including the two-electron channels explicitly in the theory over a wide photon-energy range.

INTRODUCTION

A photoelectron spectrum from atoms excited by monochromatic radiation usually reveals a number of intense lines corresponding to the one-electron excitation picture accompanied by sets of less intense peaks, the so-called satellite lines. These transitions correspond to cases in which the ion has been left in an excited state. For closed-shell atoms all satellite lines are an indication of the breakdown of the one-electron frozen-structure model and thus a manifestation of electron correlation effects.

The usually weak interactions that produce the satellite structure may under certain conditions have a strong influence on the outcome of measured physical properties of the system. In such cases it is an unavoidable necessity to include these interactions in the theory in order to get a meaningful comparison between theory and experiment. An illustrating example is the large discrepancy between theory[1] and experiment[2,3] for the Xe 5s anuglar asymmetry parameter β in the region of the Xe 5s Cooper minimum, which occurs at about 33 eV. The theoretical results[1] were based on the relativistic random-phase approximation (RRPA). This method had been shown to be very effective for the calculation of the angular asymmetry parameter β and cross sections for other subshells in rare gases.[1,4,5] However, although the RRPA calculation of the β parameter of the 5s shell includes the important interactions with the 5p and 4d subshells, it does not include two-electron channels that lead to correlation satellites in a photoelectron spectrum. On the basis of our earlier qualitative observation,[2] we considered these channels as a likely source for the existing discrepancy. This suggestion gained support by a recent paper by Wendin and Starace[6] and was emphasized more recently by the analysis of a complete spectrum recorded at one photon energy within the Cooper minimum.[7] Concurrently, Derenbach and Schmidt[8] found strong satellite contributions in a closely related case, that of the Kr 4s Cooper minimum.

In this paper we report a detailed experimental study of the Xe 5s,5p satellite spectrum at photon energies covering the Cooper minimum and reaching into the 4d delayed maximum. The data include the total and, especially, the partial strengths of the various channels. We also report on the angular asymmetry parameter β for each satellite channel. Finally, we partition the total photoionization cross section and present absolute partial cross sections for the satellites as well as for the 5s and 5p ionization channels.

EXPERIMENT

The angle-resolved experiments were carried out with an electron spectrometer designed and built at the Oak Ridge National Laboratory.[4] The photons were obtained from the storage ring Tantalus I, at Stoughton, Wisconsin and monochromatized by a toroidal grating monochromator. The resolution was affected primarily by the band pass of the monochromator which in the present photon region amounted to about 5 Å up to 50 eV and about 2 Å near 70 eV. Additional broadening comes from the electron analyzer, which has a resolution of 1% of the kinetic energy of the electron.

The differential cross section for a randomly oriented target can be expressed in terms of the angular distribution parameter β. Within the dipole approximation the parameter β can be obtained experimentally by the following relationship:

$$\beta=\frac{4(R-1)}{3P(R+1)-(R-1)}\ , \tag{1}$$

where R is $I(0°)/I(90°)$ and $I(0°)$ and $I(90°)$ are the intensities of the photoelectrons moving in the direction parallel and perpendicular to the polarization vector. The polarization P was determined from measurements on the He 1s orbital, where β is assumed to be 2.0. The photoelectron intensity was also measured as a function of the angle Θ between polarization vector and the direction of the photoelectrons resulting in an appropriate $\cos^2\Theta$ dependence and revealing a tilt of the main polarization vector out of the plane of the electron orbit. (We define the direction of this vector as the 0° direction.) In the photon-energy range used in these experiments, P was 88% to 86%.

Since our spectrometer is equipped with two electron analyzers at right angles to each other, it is possible to record simultaneously the photoelectron intensities needed for the calculation of β. These measurements are therefore insensitive to changes in the beam current or pressure variations in the source cell. However, possible changes in the response of each analyzer could give systematic errors in our β determination and calibration measurements on transitions with known β values in other rare gases were therefore performed during the progress of the experiment giving good confidence in the procedure. The relative partial cross sections for the correlation satellites were obtained by making measurements at the magic angle, which for a given polarization P is [see Eq. (1) of Ref. 4]

$$\Theta_m = \frac{1}{2}\cos^{-1}\left[-\frac{1}{3P}\right]. \tag{2}$$

Results on the relative partial cross sections were also extracted from the measured intensities by multiplying $I(0°)$ by the factor

$$\frac{1}{1+\beta(1+3P)/4}. \tag{3}$$

The results obtained in the two diffrent ways showed good consistency.

All data were taken using an 8.00 V preacceleration. The gas pressure in the source volume was in all cases between 1.0×10^{-4} and 1.5×10^{-4} Torr as measured with an electromechanical pressure transducer. The pressure in the analyzer was about 100 times lower. Although the total scattering cross section of Xe varies considerably in the energy region reported here, errors from this source were small at our operating pressure.

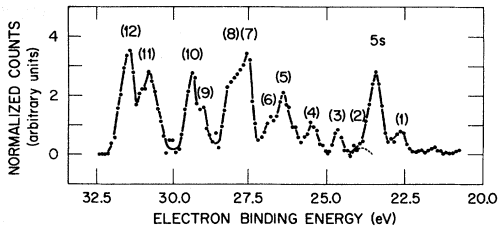

FIG. 1. Xe 5s,5p satellite spectrum. The spectrum is fully corrected as discussed in Ref. 7 and the intensities are proportional to the partial photoionization cross sections. Excitation energy was $h\nu=33$ eV.

RESULTS AND DISCUSSION

The electron spectrum from threshold up and slightly beyond the excitation of the Xe 5p doublet was recorded for nine photon energies between 28.5 and 75 eV with an emphasis on the region of the Cooper minimum. In addition, we have used data on a few satellites from our earlier work[2] on the Xe 5s angular asymmetry parameter β. The energies were selected as to avoid or minimize interference with Xe $N00$ Auger lines and 4d photolines introduced by second-order radiation. The results at 75 eV penetrate into the 4d delayed maximum and provide a tie point with the data of Adam *et al.*[9]

As a representative result of our data around the 5s Cooper minimum we show in Fig. 1 a fully corrected photoelectron spectrum of Xe obtained with 33.0 eV photon energy. As discussed in detail earlier,[7] the raw spectrum was recorded at the magic angle and, following subtraction of the background, the intensities were corrected for the variation in the spectrometer transmission and a lens

TABLE I. Observed binding energies (eV) in the Xe 5s,5p satellite spectrum and line assignments. The final satellite states quoted are of the type $5s^25p^4nl$ with even parity and $J=\frac{1}{2}$. We omit the $5s^25p^4$ notation and only include its term value.

Peak[a]	This work	1487 eV Ref. 11	75.5 eV Ref. 9	40.8 eV Ref. 12	Possible final states according to Ref. 13
5s	23.397[b]	23.40(1)	23.34(5)	23.394	$5s\,5p^6\,^2S_{1/2}$
(2)	23.9(1)			23.93(2)	
(3)	24.67(5)	24.62(5)	24.6(1)		$(^3P)6s\,^4P_{1/2}$
(4)	25.33(8)	25.24(5)	25.3(1)	25.28(2)	$(^3P)6s\,^2P_{1/2}$;$5d\,^4P_{1/2}$, $^2P_{1/2}$
(5)	26.36(5)			26.37(2)	
(6)	26.8(1)			26.63(4)	
				26.88(2)	
(7)	27.58(8)	27.95(5)	27.6(1)	27.54(2)	
(8)	28.1(1)		28.3	27.93(2)	$(^1D)5d\,^2P_{1/2}$
				28.24(4)	$(^1S)6s\,^2S_{1/2}$
(9)	28.9(1)		28.8		$(^1D)5d\,^2S_{1/2}$
(10)	29.37(5)	29.02(5)	29.3(1)		$(^3P)6d\,^4P_{1/2}$
(11)	30.7(1)				
(12)	31.4(1)	31.44(5)	31.5(1)		$(^1D)6d\,^2P_{1/2}$,$^2S_{1/2}$
	32.6(1)	32.80(5)			$(^1S)7s\,^2S_{1/2}$
		33.78(10)			

[a]Peak numbering refers to Fig. 1.

[b]Reference value according to Ref. 13.

effect arising from the preacceleration of the electrons. Hence, the intensities of the spectrum shown are directly proportional to the partial cross sections. Of the numbered lines in Fig. 1, peak 1 and most of peak 3 are Auger transitions[10] due to excitation from second-order radiation from the monochromator. These and other Auger transitions at higher kinetic energies not shown in Fig. 1 were followed closely in the earlier study[2] of the Xe 5s angular asymmetry parameter β where their relative intensities were determined for different photon energies. This enabled us in the present investigation to conclude that a previously reported satellite line[11,12] which for the photon energy of 33 eV happens to coincide with an Auger line (no. 3 in Fig. 1), must be of low intensity. However, since almost all of the numbered peaks in Fig. 1 are correlation satellites, the integral intensity of the satellites clearly indicates the importance of the satellites in this photon region where the Xe 5s has its Cooper minimum. It is also evident that many of the peaks are made up of several transitions and the numbering is therefore meant mainly to simplify referencing in the following discussion.

In Table I, the average values of the binding energies for the observed satellites are given in column 1. In addition to satellites (2)—(12) another satellite at 32.6(1) eV was observed for photon energies of 34.0 and 35.5 eV. The energies are referred to the 5s optical value.[13] Also included in Table I are data from higher photon energies, 1487 (Ref. 11) and 75.5 eV,[9] as well as high-resolution results at 40.8 eV.[12] The agreement between different data is good considering the variation in resolution in the experiments. The assignment of the lines summarized in Table I corresponds to the latest evaluation given by Hansen and Persson.[13]

As can be seen from a comparison with the He II data,[12] peaks 6 and 8 in our spectrum are probably doublets. Peak 2 has been extracted from a deconvolution based on results from the 90° recordings where the 5s peak due to its high β value decreases in intensity compared to satellite 2 which has $\beta \approx 0$. Several lines, peaks 5, 6, and 11, have not been reported in the spectra recorded at 1487 (Ref. 11) and 75.5 eV,[9] indicating that these transitions are favored only in the low-photon-energy region. (We do find a very small contribution for peaks 5 and 6 at 75 eV.) It is also interesting to note that the peaks 5 and 6 were not reported in the study of the satellite spectrum of Xe by the (e,2e) technique.[14]

The relative intensities of the main and satellite lines in the Xe 5s,5p photoelectron spectrum are given in Tables

TABLE II. Intensities of satellite lines in the Xe 5s,5p photoelectron spectrum relative to the 5s and 5s + 5p main lines for different photon energies. The intensity of the 5s line has arbitrarily been given the value 100. "Auger" indicates strong interference by Auger lines.

		Relative Intensity								
Peak[a]	Energy (eV)	28.5 eV	31.0 eV	33.0 eV	34.0 eV	35.5 eV	43.2 eV	48.3 eV	68.9 eV	74.8 eV
(5s)	23.397	100	100	100	100	100	100	100	100	100
(2)	23.9(1)	27(8)	13(4)	5(2)	Auger	8(3)				
(3)	24.67(5)	16(4)	11(3)	<5[b]	8(3)	5(2)	4(2)[c]	10(1)	11(1)	14(2)
(4)	25.33(8)	61(12)	62(15)	36(8)	56(13)[c]	Auger				
(5)	26.36(5)	102(20)	118(21)	84(15)	79(14)	83(15)	17(3)[c]	7(1)[c]	2.3(5)	1.6(4)
(6)	26.8(1)	48(9)	50(9)	33(6)	39(7)	Auger				
(7)	27.58(8)	50(9)	146(22)	113(18)	120(19)	127(20)	33(6)[c]	18(2)	12(2)	12(2)
(8)	28.1(1)		108(20)	94(15)	80(12)	42(7)				
(9)	28.9(1)		45(11)	41(7)	30(5)	33(5)	42(3)[c]	24(2)[c]	32(2)	32(2)
(10)	29.37(5)		94(20)	84(13)	73(9)	66(9)				
(11)	30.7(1)			119(27)	94(20)	44(10)	24(4)[c]	7(1)[c]	17(2)	9(2)
(12)	31.4(1)			149(34)	87(19)	61(14)				
	32.6(1)				98(23)	128(4)				3(2)
satellites to 5s		3.0(0.6)	6.5(1.0)	7.6(1.1)	7.7(1.2)	6.9(1.2)[d]	1.2(3)	0.66(5)	0.74(6)	0.72(6)
satellites to 5s + 5p		0.05(1)	0.08(1)	0.11(2)	0.14(3)	0.16(3)	0.17(5)	0.11(2)	0.22(3)	0.21(2)

TABLE III. Relative intensities of Xe 5s,5p satellites reported previously. Data at $h\nu=75$ eV are compared with our present results.

Peak	Energy (eV)	Ref. 12 40.8 eV[a]	Ref. 11 1487 eV[a]	Ref. 9 75.5 eV	This work 74.8 eV
(5s)	23.397	100	100	100	100
(2)	23.9	2(1)			
(3)	24.67		6(2)	12(2)	14(2)
(4)	25.33	5(2)	7(2)		
(5)	26.36	12(4)			1.6(4)
(6)	26.8	4(2)+5(2)[b]			
(7)	27.58	32(5)	25(4)	11(2)	12(1)
(8)	28.1	14(4)+6(2)[b]			
(9)	28.9		52(4)	34(2)	32(2)
(10)	29.37				
(11)	30.7				9(2)
(12)	31.4		20(3)	15(2)	
	32.6		6(2)		3(2)
Satellites to 5s		0.8[c]	1.16(15)[d]	0.72(8)	0.72(6)
Satellites to 5s+5p			0.21(3)	0.21(3)	0.21(2)

[a]Data recorded at 90°.
[b]Two lines were resolved with an average energy corresponding to (6) and (8).
[c]Note that no results were given for lines 9 to 12.
[d]An additional satellite was reported at 33.78(10) eV with an intensity of 0.04 relative to 5s.

II and III for our results and previous work, respectively. We also present the integrated intensity of all satellites compared to those of the 5s line and the combined 5s+5p lines. Additional data are those of Southworth *et al.*,[15] who report a satellite-to-5s intensity ratio of about 1.0 at 63 eV and the magic angle, and Spears *et al.*[16] who report a ratio of 0.73(8) at 1487 eV and 90°.

Several observations can be made by examining these tables. For photon energies between 31 and 35.5 eV the total satellite intensity as compared to the 5s peak is nearly 10 times greater than at higher energies, $h\nu \gtrsim 45$ eV, and the total satellite intensity exceeds the 5s intensity by a factor of ≈ 7. However, when compared to the combined 5s+5p line intensity, the total satellite intensity is smaller than it is for high photon energies. When compared within the photon range of the present study, the satellite-to-5s+5p intensity is steadily decreasing toward lower photon energy from a high-energy plateau that begins at about 70 eV. A rapid drop in the relative satellite intensity seems to occur in the neighborhood of 40 eV; unfortunately, the strong interference of Auger lines in this energy region prevented us from delineating the transition region in detail. As seen from Table III our results and those by Adam *et al.*[9] are in generally very good agreement at $h\nu=75$ eV chosen by both groups. We also list the results reported by Süzer and Hush[12] and by Gelius[11] although their data were recorded at 90°, which results in a decreased satellite-to-5s intensity ratio due to the strong peaking of the 5s signal in the 90° direction ($\beta \approx 2$) for the unpolarized photons used in that work.[11,12] If we were to assign as much strength to the unreported lines 9 to 12 as to the measured lines, the relative satellite intensity at 40.8 eV would lie between 1.6 and 3.2 in the limits of the possible β values. A likely value around 2 for the corrected 90° results would then fit in nicely with our results at the magic angle which are true relative intensities. The values for $h\nu=1487$ eV would also increase and, hence, overshoot the values measured at 75 eV. If we assumed an average β value of 1 for the satellites, the satellite intensity referred to 5s would be less than 1 according to Spears *et al.*[16] and about 1.4 according to Gelius.[11] However, the intensity referred to that for 5s+5p would increase by only about 5% because of the much larger 5p intensity.

While the identification of the processes that lead to the satellite lines can often be done on the basis of an energy determination, the dynamic behavior including the specific interactions of these two-electron processes with single-electron processes can be evaluated most profitably from the cross sections and photoelectron angular distri-

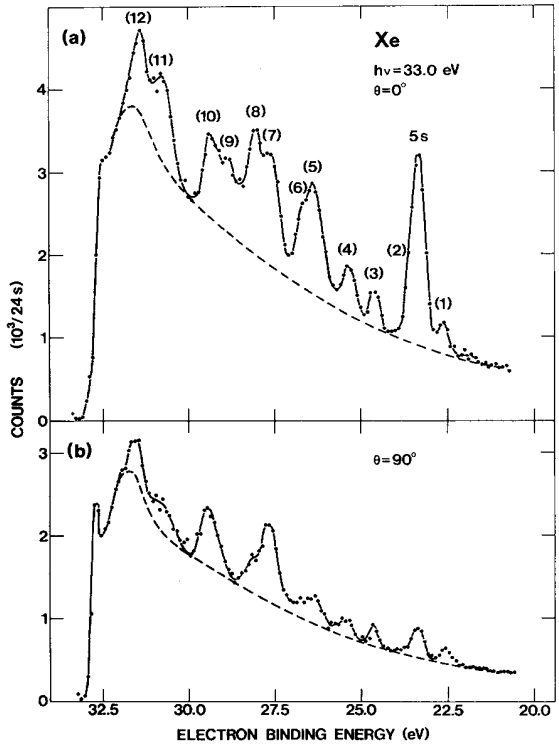

FIG. 2. Xe $5s,5p$ satellite spectrum, including the $5s$ photoline, as recorded at the angle $\Theta=0°$ (upper panel) and $\Theta=90°$ (lower panel). The spectra clearly demonstrate the angular dependence for the different features. Photon energy was $h\nu=33$ eV; and the dashed lines give the estimated background. The numbering of the peaks is the same as in Fig. 1.

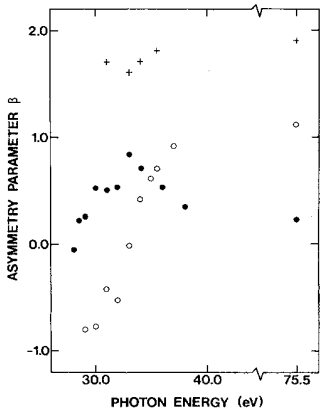

FIG. 3. Figure shows the variation in the angular asymmetry parameter β for the satellites 5, 7, and 9. The solid circles (●) represent satellite 5, open circles (○) satellite 7 and plus signs (+) represent satellite 9. No β values were measured between 40 and 70 eV. Note the similarity of the β curve for line 9 with that for the $5s$ photoline of Refs. 2 and 3.

butions. We discuss the angular distributions first.

As an illustrative example of the change in the structures with the angle Θ we present in Fig. 2 photoelectron spectra recorded at 0° and 90°, respectively. The exciting photon energy is 33.0 eV and the energy region is the same as the one shown in Fig. 1. The spectra in Fig. 2 are not corrected for spectrometer dispersion and differences in response. It is nevertheless very obvious that the $5s$ line and satellite 9 must have a high β value whereas, for example, satellite 7 must correspond to a β value close to 0. The dashed lines in the spectra are our estimates of the background from threshold up and slightly beyond the main $5s$ peak. The background changes with angle and the two analyzers have different response functions, and both effects are most clearly seen close to threshold. As in the case of the spectra recorded at the magic angle we used information from spectra excited by neighboring photon energies in the process of assigning a proper background.

The β values measured for five photon energies are given in Table IV, and the β values of three satellites are plotted in Fig. 3. Several data points not represented in the tables were also incorporated in the plots. We see that satellite 9 has a very high β value for all photon energies and a dip near 33 eV reminiscent of the β curve for Xe $5s$.[2,3] The satellite is suggested[13] to be an example of the well-known final-state configuration interaction between the $5s\,5p^6$ and $5s^2 5p^4 5d$ configurations. In this case it is $5s^2 5p^4(^1D)5d\,^2S_{1/2}$ which would be most strongly interacting with $5s\,5p^6\,^2S_{1/2}$. Since both transitions show a

TABLE IV. Values for the angular distribution parameter β for the Xe $5s,5p$ correlation satellites as a function of photon energies around the Xe $5s$ Cooper minimum.

	Photon energy (eV)				
Peak[a] (eV)	28.5	31.0	33.0	34.0	35.5
(2) 23.9	0.19(10)	0.18(12)	0.04(10)		
(3) 24.67	0.28(11)			0.22(13)	
(4) 25.33	0.10(12)	0.05(7)	0.59(7)		
(5) 26.36	0.21(8)	0.49(8)	0.83(10)	0.70(9)	0.61(10)
(6) 26.8	0.18(9)	0.76(10)	0.83(8)	0.42(14)	
(7) 27.58	−0.8(1)	−0.43(8)	−0.02(8)	0.42(10)	0.70(10)
(8) 28.1		0.44(10)	0.50(10)	0.59(10)	0.71(10)
(9) 28.9		1.70(10)	1.60(10)	1.70(10)	1.80(10)
(10) 29.37		0.0(1)	0.10(10)	0.23(10)	0.42(10)
(11) 30.7			0.41(9)	0.60(10)	
(12) 31.4			0.4(1)	0.4(1)	
32.6				−0.3(1)	

[a]Peak numbering refers to Figs. 1 and 2.

TABLE V. Partial cross sections (Mb) as a function of photon energy. Quoted errors do not include uncertainties in the absolute photoionization cross sections which are given in the last row.

	Photon energy (eV)									
Peak[a]	28.5	31.0	33.0	34.0	35.5	43.2	48.3	68.9[b]	74.8	1487[c]
$5p$	9.0(3)	6.0(2)	4.2(1)	3.4(1)	2.6(1)	1.1(2)	0.87(5)	0.37	0.70(6)	0.30
$5s$	0.14(2)	0.07(1)	0.06(1)	0.06(1)	0.06(1)	0.17(5)	0.17(3)	0.16	0.29(4)	0.06
(2)	0.04(1)	0.009(3)	0.003(1)	d	0.005(2)					
(3)	0.023(6)	0.008(2)	0.003(1)	0.005(2)	0.003(1)	0.008(5)	0.017(3)	0.02	0.042(6)	0.01
(4)	0.09(2)	0.04(1)	0.023(5)	0.034(8)	d					
(5)	0.15(3)	0.08(2)	0.05(1)	0.05(1)	0.05(1)	0.03(1)	0.011(3)	0.004	0.005(2)	
(6)	0.07(1)	0.036(6)	0.021(4)	0.024(4)	d					
(7)	0.07(1)	0.10(2)	0.07(1)	0.07(1)	0.08(1)	0.06(2)	0.030(5)	0.02	0.036(8)	0.017
(8)		0.08(1)	0.06(1)	0.049(8)	0.026(5)					
(9)		0.032(8)	0.026(4)	0.018(3)	0.020(3)	0.07(2)	0.041(6)	0.05	0.094(12)	0.034
(10)		0.07(1)	0.054(8)	0.045(6)	0.040(6)					
(11)			0.08(2)	0.06(1)	0.03(1)	0.04(1)	0.011(3)	0.03	0.026(5)	0.013
(12)			0.10(2)	0.06(1)	0.04(1)					
Satellites to (1)–(12)	0.44	0.46	0.48	0.41	0.37	0.21	0.11	0.12	0.20	0.08
σ(tot)	9.62	6.52	4.80	4.12	3.37	1.82	1.58	3.89	8.4	0.89

[a]Peak numbering refers to Fig. 1.
[b]The values in this column are very uncertain because of the problem of reliably extrapolating the $4d$ cross section; our estimate is $\sigma(4d)=2.0$ Mb.
[c]From Ref. 11; these values which are not corrected for the angular distribution (β) are given for the purpose of a rough comparison.
[d]Strong interference by Auger lines.

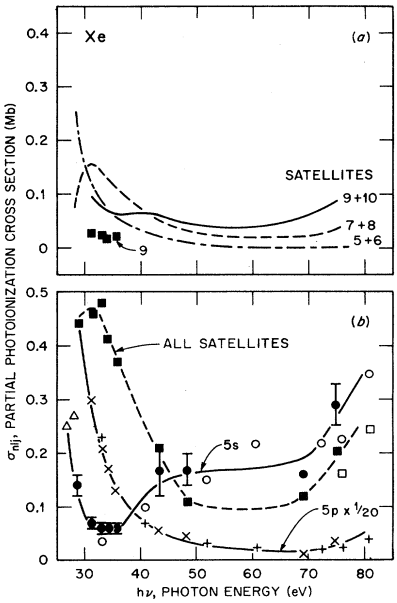

FIG. 4. Partial photoionization cross sections for the $5s$ and $5p$ single-electron emission processes and the sum of all two-electron processes that produce photoelectron correlation satellites (lower panel) and for a number of two-electron processes leading to the satellites indicated (upper panel). For clarity the actual points given in Table V are omitted in panel (a), except for line 9. In panel (b), our data and Adam *et al.*'s results (Refs. 9 and 19) are shown, respectively, for $\sigma(5p)$ as ($\times$) and ($+$), for $\sigma(5s)$ as ($\bullet$) and ($\circ$), for σ(all sat) as ($\blacksquare$) and ($\square$); in addition ($\triangle$) for $\sigma(5s)$ from Ref. 20.

similar behavior one gets further support for the identification of satellite 9. Another interesting feature is satellite 7, so far unidentified. It changes its β values very rapidly over a narrow energy range, going from almost -1 near threshold to above $+1$ at 75 eV. Satellite 5 has a maximum in its β value when the photon energy is scanned through the Xe $5s$ Cooper minimum. It follows the same pattern as β for the Xe $5p$ photoelectron,[4] except that the β maximum is not as high as for Xe $5p$ ($\beta_{\max}=1.8$).

The absolute partial cross sections for the $5p$,$5s$ photolines and their attending satellites are displayed in Fig. 4 and Table V. These values were obtained by partitioning the total photoionization cross section given by West and Morton.[17] The relative intensities of Table II provided the needed input together with the results for double ionization presented by Adam[19] and, where applicable, the relative $4d$ photoelectron intensities.[18] Triple ionization was neglected.

Viewing Fig. 4(b), we first draw attention to the Cooper minimum in $\sigma(5s)$ and the subsequent rise of $\sigma(5s)$ toward the $4d$ delayed maximum occurring at 100 eV. By contrast, $\sigma(5p)$ drops rapidly from a high value near threshold and experiences an enhancement starting near 70 eV. Our data are in good accord with previous determinations,[18] and we show for comparison the points of Adam *et al.*[9,19] and Samson and Gardner.[20] The total satellite cross section, σ(sat), is seen to slightly rise through the Cooper minimum. Then it decreases rapidly although not quite as steeply as $\sigma(5p)$. Finally, σ(sat) rises at the onset of the $4d$ delayed maximum in a similar manner as does $\sigma(5s)$.

Partial cross sections for several satellite pairs are plotted in Fig. 4(a). To a large extent, the choice of the pairs was dictated by the obvious spectral features, as seen in Fig. 1. Nevertheless the plots reveal characteristics attributable to at least one of the satellites. Satellites 5 and 6 follow the behavior of the $5p$ electrons suggesting as does the angular distribution parameter β (Fig. 3 and Table IV) that these satellites are closely related with the $5p$ subshell. Satellites 7 and 8 display a mixed and somewhat unusual trend in σ as line 7 does in β. A pronouced drop in σ is observed close to threshold (see also Table II). The cross section of satellites 9 and 10 shows a definite similarity with $\sigma(5s)$, corroborating the finding for the β parameter of the line 9. In the Cooper minimum, σ(sat 9) has the same behavior as $\sigma(5s)$.

CONCLUSIONS

The results of this work establish the high intensity of the correlation satellites reported previously[7] for $h\nu=33$ eV over the entire extent of the Xe $5s$ Cooper minimum. The absolute partial cross sections that were obtained for all components of the Xe $5s$,$5p$ photoelectron spectrum demonstrate clearly the similar behavior of the properties of the processes that lead to the $5s5p^6\,^2S_{1/2}$ and $5s^25p^4(^1D)5d\,^2S_{1/2}$ final ionic states. These states couple strongly, and the present experimental data will provide a testing ground for theoretical models that will include explicitly this important interaction. Other satellites were shown to be closely associated with the $5p$ ionization channel. However, since there is considerable interchannel interaction[1] between $5p$ and $5s$, these satellites will in turn have an effect on the dynamic parameters of the $5s$ electrons. Considerations of all intense two-electron processes appears therefore essential to improve the theoretical predictions of the Xe $5s$ β parameter in the Cooper minimum.

Although the satellite intensities were not investigated over the entire $4d$ delayed maximum, the occurrence of an enhancement of their cross section in this region was demonstrated. A discrepancy between theory and experiment for $\sigma(5s)$ was reported earlier.[9,19] One might expect, however, that detailed considerations of the satellite transitions would remove the differences.

As seen from Table I satellites 2, 5, 6, 7, and 11 cannot be explained with the same type of configuration interaction as in the case of satellite 9 and others. In analogy with the satellite structure of argon[21] one could allow for a mixing of configurations like $5p^4mlm'l'$ with the ground-state configuration $5p^6$ to describe the initial state more properly. This would open up new possibilities for final states. For xenon, transitions with final states like $5s^25p^4(^3P)5d\,^2P,^2D,^2F,^4D$ as well as $5s^25p^4(^3P)6p\,^2P,^2D,^4D$ would be allowed. A comparison with optical data[13] shows that these final states have energies that may convolute to the unidentified satellites 5, 6, and 7. However, no optical information is available for

the identification of satellites 2 and 11.

Finally, we point out the different behavior of the satellites at low energies as compared with that at high photon energies. These differences are especially strong, and may vary from satellite to satellite, if strong many-electron interactions, including interchannel coupling, are present as in the case of xenon. But even with weaker interactions, the low energy or near-threshold behavior cannot be predicted from high-energy data as was demonstrated previously for He (Refs. 22–24) and Ne.[24–26]

ACKNOWLEDGMENTS

This research was sponsored by the Division of Chemical Sciences, Office of Basic Energy Sciences, U. S. Department of Energy under Contract No. W-7405-eng-26 with the Union Carbide Corporation. The Synchrotron Radiation Center at Stoughton, Wisconsin, is operating under National Science Foundation Grant No. DMR-80-20164.

*On leave from Department of Physics and Measurement Technology, Linköping Institute of Technology, S-581 83 Linköping, Sweden.

†On leave from Royal Institute of Technology, S-100 44 Stockholm, Sweden.

[1]W. R. Johnson and K. T. Cheng, Phys. Rev. A **20**, 978 (1979).

[2]A. Fahlman, T. A. Carlson, and M. O. Krause, Phys. Rev. Lett. **50**, 1114 (1983).

[3]H. Derenbach and V. Schmidt, J. Phys. B **16**, L337 (1983).

[4]M. O. Krause, T. A. Carlson, and P. R. Woodruff, Phys. Rev A **24**, 1374 (1981).

[5]S. H. Southworth, Ph.D. thesis, Lawrence Berkeley Laboratory, University of California, 1982.

[6]G. Wendin and A. F. Starace, Phys. Rev. A **28**, 3143 (1983).

[7]A. Fahlman, M. O. Krause, and T. A. Carlson, J. Phys. B **17**, L217 (1984).

[8]H. Derenbach and V. Schmidt, J. Phys. B **17**, 83 (1984).

[9]M. Y. Adam, F. Wuilleumier, N. Sandner, V. Schmidt, and G. Wendin, J. Phys. (Paris) **39**, 129 (1978).

[10]L. O. Werme, T. Bergmark, and K. Siegbahn, Phys. Scr. **6**, 141 (1972); values adjusted according to Ref. 13.

[11]U. Gelius, J. Electron Spectrosc. **5**, 984 (1974).

[12]S. Süzer and N. S. Hush, J. Phys. B **10**, L705 (1977).

[13]J. E. Hansen and W. Persson, Phys. Rev. A **18**, 1459 (1978).

[14]S. T. Hood, A. Hamnett, and C. E. Brion, J. Electron Spectrosc. **11**, 205 (1977).

[15]S. H. Southworth, U. Becker, C. M. Truesdale, P. H. Kobrin, P. W. Lindle, S. Owaki, and D. A. Shirley, Phys. Rev. A **28**, 261 (1983).

[16]D. Spears, E. J. Fishbeck, and T. A. Carlson, Phys. Rev. A **9**, 1603 (1974).

[17]J. B. West and J. Morton, At. Data Nucl. Data Tables **22**, 103 (1978).

[18]M. O. Krause, in *Synchrotron Radiation Research,* edited by H. Winick and S. Doniach (Plenum, New York, 1980), Chap. 5, p. 101. This article summarizes the available results.

[19]M. Y. Adam, Ph.D. thesis, L'Université de Paris—Sud, Centre d'Orsay, France, 1978.

[20]J. A. R. Samson and J. L. Gardner, Phys. Rev. Lett. **33**, 671 (1974).

[21]M. Y. Adam, F. Wuilleumier, S. Krummacher, V. Schmidt, and W. Mehlhorn, J. Phys. B **11**, L413 (1978).

[22]K. A. Berrington, P. G. Burke, W. G. Fon, and K. T. Taylor, J. Phys. B **15**, L603 (1982).

[23]P. Morin, M. Y. Adam, I. Nenner, J. Delwiche, M. J. Hubin-Franskin, and P. Lablanquie, Nucl. Instrum. Meth. **208**, 761 (1983).

[24]K. G. Dyall and F. P. Larkins, J. Phys. B **15**, 219 (1982).

[25]F. Wuilleumier and M. O. Krause, Phys. Rev. A **10**, 242 (1974).

[26]P. H. Kobrin, S. Southworth, C. M. Truesdale, D. W. Lindle, U. Becker, and D. A. Shirley, Phys. Rev. A **29**, 194 (1984).